The Peroxidasic Activity of the Haem Octapeptide Microperoxidase-8 (MP-8): The Kinetic Mechanism of the Catalytic Reduction of H_2O_2 by MP-8 using 2,2'-Azinobis-(3-ethylbenzothiazoline-6-sulphonate) (ABTS) as Reducing Substrate

Paul A. Adams
MRC Biomembrane Research Unit, Department of Chemical Pathology, University of Cape Town Medical School, Observatory 7925, Cape Province, Republic of South Africa

Kinetic studies of the MP-8-catalysed reduction of H_2O_2 using the chromophoric reducing substrate, ABTS, are reported. Over a wide range of MP-8, H_2O_2, and ABTS concentrations—under the conditions [ABTS] > 10 $[H_2O_2]$ > 10 [MP-8]—the formation of the $ABTS^{+\bullet}$ cation radical adheres precisely to a first-order kinetic rate law over at least 90% reaction. Kinetic studies using cyclical variation of the concentration of each reactant under conditions where the concentrations of the other two were maintained constant revealed that the pseudo-first-order rate constant is a sum of three independent terms, implying three parallel kinetic processes. These processes are suggested to be:

(i) a 'normal' peroxidase-type catalytic cycle with free MP-8 as the catalyst, proceeding *via* hypervalent oxo-iron(IV) porphyrin intermediates, analogous to compounds I and II of the peroxidase enzymes;

(ii) a parallel cycle to (i) in which the catalyst is an MP-8·ABTS complex, as opposed to the free MP-8 of (i); and

(iii) a degradative process involving direct attack of H_2O_2 on the MP-8 porphyrin moiety. This degradative pathway is inhibited by ABTS in a manner which indicates that only MP-8, *not* the MP-8·ABTS complex, is susceptible to attack by H_2O_2.

The relevant kinetic parameter for the mechanistic study of iron-porphyrin peroxidasic model systems using ABTS is thus suggested to be the limiting first-order rate constant as both [ABTS] and $[H_2O_2]$ tend to zero.

The reaction between hydrogen peroxide and iron-porphyrins has been intensively studied as a chemical model for the peroxidase and catalase enzymes—haem proteins which catalyse reactions (1) and (2), respectively.

$$2RH + H_2O_2 \xrightarrow{\text{Peroxidase}} 2H_2O + 2R \quad (1)$$

(RH = Reducing substrate)

$$2H_2O_2 \xrightarrow{\text{Catalase}} 2H_2O + O_2 \quad (2)$$

Initially the reaction between simple iron-porphyrins such as proto-, deutero-, haemato-ferrihaem, *etc.* and H_2O_2 was investigated in aqueous solution;[1,2] however, such studies, despite yielding invaluable information concerning reactions (1) and (2) above, suffer from three major drawbacks:

(i) the iron-porphyrin catalysts may aggregate extensively in aqueous solution;[3]

(ii) H_2O_2/active oxygen species react non-catalytically with the porphyrin, causing macrocycle degradation (alternatively, reactive iron oxo intermediates formed react between themselves with resultant catalyst destruction); and

(iii) the major protein-derived contribution to the chemical state of the catalytic iron centre in the enzymes—namely the proximal imidazole of a histidine—is absent in the simple iron-porphyrins studied.

An elegant approach circumventing these problems has been developed in recent years by Traylor *et al.*[4] who have investigated the kinetics and mechanism of reactions between peroxo species and 'tailbase' porphyrins in non-aqueous solution, using tri-t-butylphenol to trap hypervalent iron oxo radical species (peroxidase compound 1 analogues).[4,5] This considerably reduced catalyst destruction, and catalytic turnover numbers as high as 5×10^4 were achieved.[5] 2,2'-Azinobis-(3-ethylbenzothiazoline-6-sulphonate) (ABTS) has been used for a number of years as a simple chromogenic reducing substrate for the peroxidase enzymes.[6] The reaction of horseradish peroxidase (HRP) with H_2O_2 results in two molecules of ABTS being oxidised (by HRP compounds I and II successively) for each molecule of H_2O_2 metabolised, the kinetics of the reaction being conveniently monitored by formation of the emerald green $ABTS^{+\bullet}$ cation radical which absorbs in the visible region at 660 nm. Bruice and co-workers have used ABTS as a radical trap to investigate the mechanism of reaction between peroxo species and a monomeric, non-μ-oxo-dimer-forming, iron-porphyrin— 5,10,15,20-tetrakis-(2,6-dimethyl-3-sulphophenyl)-porphinato-iron(III) hydrate—in aqueous solution;[7,8] the porphyrin catalyst in this system, however, does not possess the imidazole of the tailbase porphyrins—a model for the proximal histidine of the enzymes.

The haem peptides derived from cytochrome-*C* (MP-) have long been known to possess peroxidasic activity,[9,10] a property which has found practical application in cell biology and histochemistry.[11,12] Marques has recently carried out a comprehensive study of the aqueous/aqueous-organic solution chemistry of the octapeptide MP-8[13] (including aspects of the peroxidasic reaction of the peptide);[14] in addition it has been demonstrated that the peptide is essentially monomeric in aqueous solution at

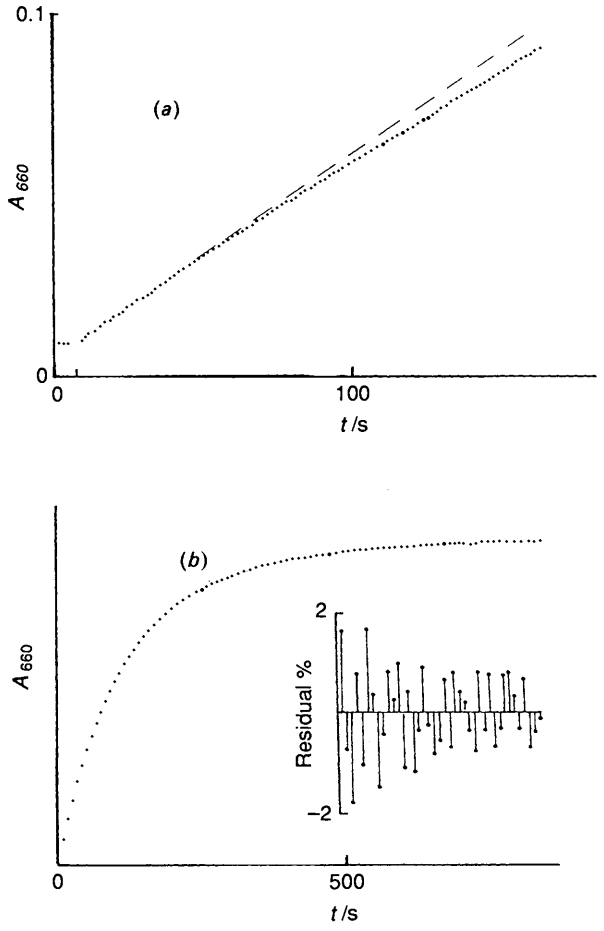

Figure 1. (*a*) Experimental determination of initial reaction rate—the initial rate from the quadratic fit to the data is shown as the dashed line in the Figure. [MP-8] 2.0×10^{-7} mol dm^{-3}; [ABTS] 5×10^{-3} mol dm^{-3}; [H_2O_2] 1×10^{-4} mol dm^{-3}. (*b*) First-order kinetic trace at [ABTS] 1×10^{-3} mol dm^{-3}; [MP-8] 5.08×10^{-7} mol dm^{-3}; [H_2O_2] 1×10^{-4} mol dm^{-3}. Residuals for the first 40 data points are shown. The least-squares value for k_{obs} was 7.49 ($\pm$0.04) $\times 10^{-3}$ s^{-1}.

catalytic concentrations ($< 10^{-6}$ mol dm^{-3}).[15] Furthermore, at neutral pH in aqueous solution the imidazole of His 18 (cyt-c sequence numbering) occupies the fifth co-ordination position of the iron,[16] providing an analogue for the proximal histidine of the enzyme. It would seem therefore that MP-8 is an ideal compound with which to combine the advantages offered by the approaches of Traylor and Bruice respectively to investigate the nature of oxo-intermediates formed on reaction with H_2O_2 in aqueous solution, utilising ABTS as a convenient radical trap to monitor the kinetics of the process.

We report here the use of ABTS to elucidate the kinetic mechanism of the catalytic reduction of H_2O_2 by MP-8 in aqueous solution at pH 7.00. It is shown that an oxo-iron(IV)-porphyrin cation radical species—a peroxidase compound I analogue—is formed during the reaction. Direct kinetic evidence is presented which indicates that a major route for oxidative macrocycle degradation occurs in the system by direct attack of H_2O_2 (or H_2O^-) on the porphyrin and that this degradative pathway is blocked by formation of an ABTS·MP-8 complex, which itself possesses a peroxidasic catalytic competency *ca.* one-third that of free MP-8.

A preliminary report of aspects of this study has been published.[17]

Experimental

H_2O_2 (100 vol) was ex BDH (Poole, UK) Analar grade; the concentration of H_2O_2 stock solution was determined spectrophotometrically (ε_{240} 39.4 mol^{-1} dm^3 cm^{-1}).[18] ABTS (Sigma Chemical Co., St Louis, Mo) was used without further purification. MP-8 (>99%) was prepared from horse heart cytochrome-c by the optimised procedure described recently,[19] the concentration of stock solutions being measured spectrophotometrically (ε_{395} 98 300 mol^{-1} dm^3 cm^{-1} at pH 11.0).[15] Phosphate buffers (0.10 mol dm^{-3}) were made up to pH 7.00, and the pH was again adjusted to 7.00 with KOH, after preparation of ABTS stock solution, immediately prior to use.

The reaction of H_2O_2 with MP-8 was monitored by following the appearance of the ABTS$^{+\bullet}$ cation radical at 660 nm, using a Varian 635 UV–visible spectrophotometer calibrated for absorbance linearity and accuracy as previously described.[20] Absorbance–time data were digitised by interfacing a Hewlett-Packard HP-85 microcomputer with the output of the spectrophotometer *via* a Hewlett-Packard 3438A digital multimeter. In a typical experimental run a solution of MP-8 ($1–10 \times 10^{-7}$ mol dm^{-3}) and ABTS (0.0001–0.010 mol dm^{-3}) was held in a cuvette at 25 °C ($\pm$0.02 °C) in the spectrophotometer cell compartment, and the reaction was initiated by addition, with mixing, of stock H_2O_2 solution (3×10^{-6} to 2×10^{-4} mol dm^{-3} final concentration). Absorbance values were sampled at fixed time intervals with up to 500 data points being obtained per run [Figure 1(*a*) and (*b*)]. Data were analysed directly either by non-linear least-squares fitting to the general first-order equation or, for initial

$$\text{Abs} = \text{A} + \text{B}^{-k_{obs}t} \quad (3)$$

velocity studies (conducted over the first 5% reaction) by fitting to the quadratic equation (4)

$$\text{Abs} = \text{A} + \text{B}t + \text{C}t^2 \quad (4)$$

Parameter errors ($\pm$1 SD) were obtained in each case and the distribution of residuals was used to assess the validity of the model equation fitted.

Spectrophotometric titrations were carried out using Helma dual-compartment mixing cells and a Hewlett-Packard HP-8450 Diode Array spectrophotometer for differential precision spectrophotometric measurements where the background absorbance was high (up to 4 AU). Results were obtained at an ambient temperature of 25 °C $\pm$ 1 °C in an unthermostatted cell holder.

Microlitre (mm^3) syringes were checked for accuracy and reproducibility of repeat volume dispensation by measuring weights of pure water delivered using a five-decimal-place balance. The reproducibility of delivery of 5 mm^3 amounts was better than $\pm$0.4%.

Temperature control was effected using a Colora cryothermostat bath to circulate constant-temperature water ($\pm$0.01 °C) around the cuvette holder. Cuvette cell-content temperature was checked using a thermistor sensitive to $\pm$0.01 °C, and calibrated using standard thermometers and the ice–water transition. Particular care was taken to ensure thermal equilibration prior to initiation of reaction; addition of reactants (normally 1–10 mm^3) to thermally equilibrated cell contents (3 cm^3) followed by mixing with a plastic platen perturbed the temperature by <0.02 °C in blank runs. Temperature accuracy and precision in this work is thus of the order of 0.02 °C.

Results

Typical absorbance–time traces for the reaction are shown in Figure 1. ABTS$^{+\bullet}$ formation followed pseudo-first-order

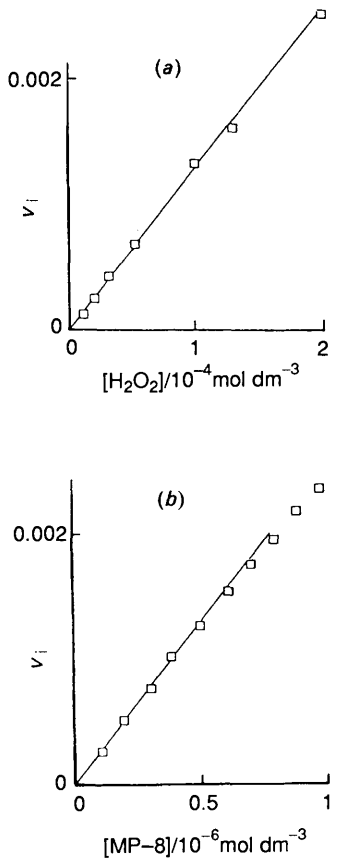

Figure 2. (*a*) Initial velocity *vs.* $[H_2O_2]$ at [MP-8] 5×10^{-7} mol dm^{-3}; [ABTS] 5×10^{-3} mol dm^{-3}. (*b*) Initial velocity *vs.* [MP-8] at $[H_2O_2]$ 1×10^{-4} mol dm^{-3}; [ABTS] 5×10^{-3} mol dm^{-3}; the slight curvature at [MP-8] $> 7 \times 10^{-7}$ mol dm^{-3} is most probably due to aggregation—see the text.

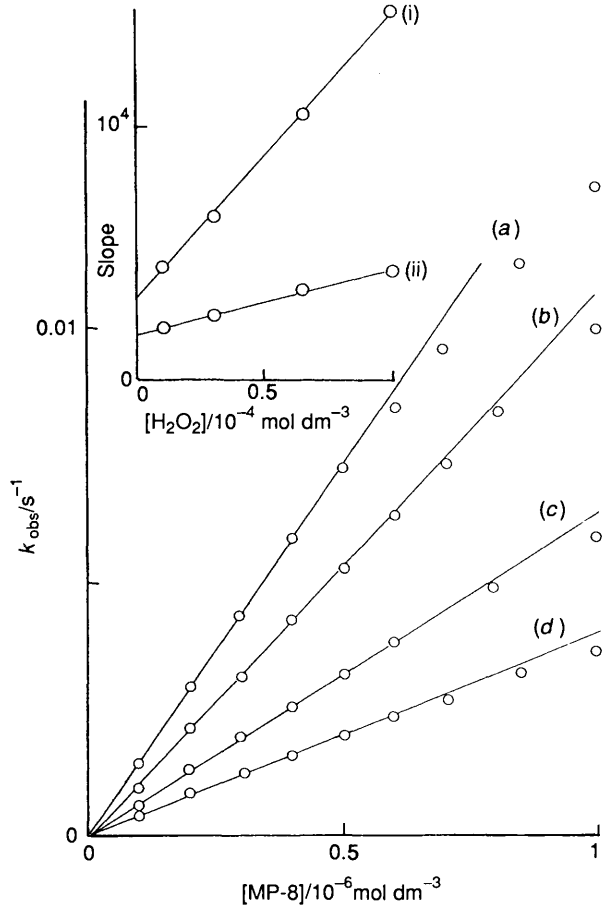

Figure 3. Variation of k_{obs} with [MP-8] at four $[H_2O_2]$-values [1.0×10^{-4}; 6.5×10^{-5}; 3.0×10^{-5}; and 1.0×10^{-5} mol dm^{-3} are data sets (*a*)–(*d*), respectively] and [ABTS] 1.0×10^{-3} mol dm^{-3}. The inset (i) shows the straight-line dependence of the slope of these lines evaluated in the region 5×10^{-7} mol dm^{-3} > [MP-8] > 0. Inset data (ii) is single-point slope evaluation (assuming k_{obs} 0 at [MP-8] 0) at [MP-8] 5.0×10^{-7} mol dm^{-3} for [ABTS] 5.0×10^{-3} mol dm^{-3}.

kinetics to >90% reaction over the whole of the concentration ranges studied. The precision of the pseudo-first-order rate constant determination was assessed by carrying out ten repeat determinations of k_{obs} at [MP-8] 5×10^{-7} mol dm^{-3}; $[H_2O_2]$ 2×10^{-5} mol dm^{-3} and [ABTS] 1×10^{-3} mol dm^{-3}. The mean value for k_{obs} was found to be 2.642×10^{-3} s^{-1} with a standard deviation of 0.019; we therefore consider that the precision of the rate constants obtained in this work is of the order of 1%.

The efficiency of the catalytic process was calculated from the known concentration of H_2O_2 used, and the value of $\varepsilon_{660}(ABTS^{+\bullet})$ 1.47×10^4 dm^3 mol^{-1} cm^{-1} measured here using standard H_2O_2 and HRP; this value compared well with that of 1.4×10^4 dm^3 mol^{-1} cm^{-1} reported in the literature.[21] The efficiency is expressed relative to that for the HRP-catalysed process being 200% (*i.e.* $2ABTS^{+\bullet}$ formed per H_2O_2 metabolised) and is calculated as given in equation (5).

$$\text{Efficiency (\%)} = \frac{\text{Total}\Delta A_{660} \times 100}{[H_2O_2] \times 1.47 \times 10^4} \quad (5)$$

Thus a calculated efficiency of 100% reflects oxidation of one $ABTS^{+\bullet}$ (average) per catalytic cycle; this parameter is important in this and subsequent work—see the Discussion section.

The following summarise the kinetic results obtained under the concentration conditions: [ABTS] ≫ $[H_2O_2]$ ≫ [MP-8].

(i) The initial velocity of $ABTS^{+\bullet}$ formation is directly proportional to $[H_2O_2]$ at constant [MP-8]; and *vice versa* [Figure 2(*a*) and (*b*)]. The apparent second-order rate constant calculated from the data shown, using equation (6), was 1 731

$$d[ABTS^{+\bullet}]/dt = k_2[MP\text{-}8][H_2O_2] \quad (6)$$

(±29) dm^3 mol^{-1} s^{-1} [Figure 2(*a*)], and 1 742 (±41) dm^3 mol^{-1} s^{-1} [Figure 2(*b*)].

(ii) At constant [ABTS] and $[H_2O_2]$, k_{obs} was directly proportional to [MP-8] (Figure 3) in the concentration region 0 < [MP-8] < 5×10^{-7} mol dm^{-3}. Significant deviation from direct proportionality was observed for [MP-8] > 6×10^{-7} mol dm^{-3}. At constant [ABTS] a plot of the slope of the k_{obs} *vs* [MP-8] plots showed a straight line against $[H_2O_2]$ (inset to Figure 3). The least-squares regression lines obtained at the two [ABTS] investigated are shown in equations (7) and (8).

[ABTS]

1×10^{-3} mol dm^{-3} $\quad sl = 1.12 \times 10^8 [H_2O_2] + 3\,160 \quad (7)$

5×10^{-3} mol dm^{-3} $\quad sl = 2.70 \times 10^7 [H_2O_2] + 1\,700 \quad (8)$

(iii) At constant [MP-8] and [ABTS] the pseudo-first-order rate constant, k_{obs} varied in an accurately straight-line manner with $[H_2O_2]$ (Figure 4). The intercept (k_0) at $[H_2O_2]$ 0, and the slope (sl) of the lines—obtained from linear

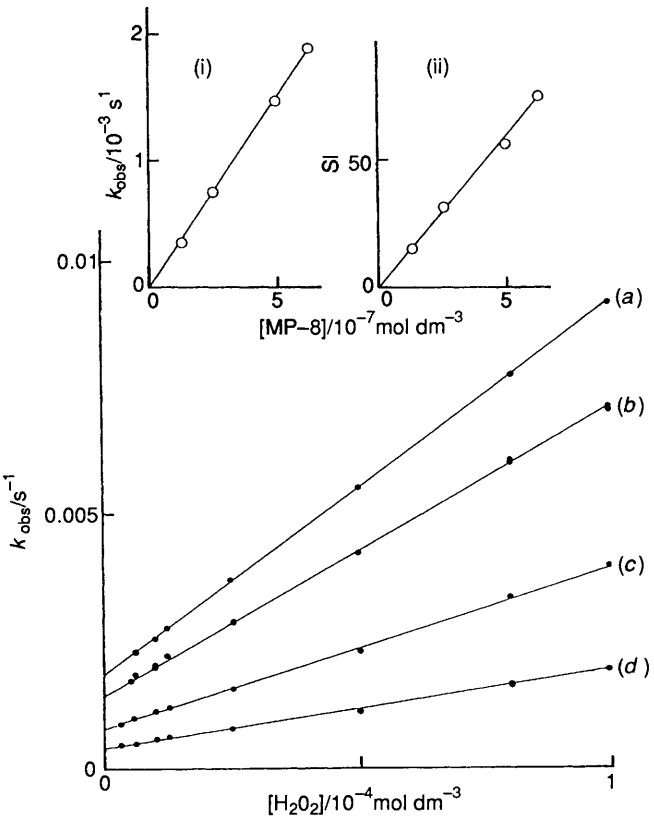

Figure 4. Plots of k_{obs} *vs.* [H_2O_2] at a number of fixed [MP-8] with [ABTS] 1 × 10^{-3} mol dm^{-3}. Data sets (*a*)–(*d*) are [MP-8] 6.23 × 10^{-7}; 4.97 × 10^{-7}; 2.69 × 10^{-7}; and 1.247 × 10^{-7} mol dm^{-3} respectively. The insets (i) and (ii) illustrate the direct proportionality of intercept (k_0) and slope (sl) of the plots to [MP-8].

Table. The effect of bromide and formate ions on the MP-8-catalysed reduction of H_2O_2.

(i) [Br^-]/mol dm^{-3}	$k_{obs}/10^{-3}$ s^{-1}	% Eff.
0	2.26	109
0.025	2.51	104
0.050	2.89	103
(ii) [HCO_2^-]/mol dm^{-3}	**$k_{obs}/10^{-3}$ s^{-1}**	**% Eff.**
0	3.29	40.6
0.05	3.24	39.4
0.10	3.36	40.2

(i) [MP-8] 5 × 10^{-7} mol dm^{-3}; [ABTS] 5 × 10^{-4} mol dm^{-3}; [H_2O_2] 5 × 10^{-6} mol dm^{-3}. (ii) [MP-8] 2.5 × 10^{-7} mol dm^{-3}; [ABTS] 5 × 10^{-4} mol dm^{-3}; [H_2O_2] 5 × 10^{-5} mol dm^{-3}.

least-squares analysis of the data in Figure 4—were both found to be directly proportional to [MP-8]: this is shown in the inserts to Figure 4, the best straight-line fit to the data of the inserts gives values calculated by equation (1) and (10).

$$k_0 = 2\,963\,(\pm 161)\,[\text{MP-8}] + 0.000\,02\,(\pm 0.000\,02) \quad (9)$$

$$\text{sl} = 1.188\,(\pm 0.072) \times 10^8\,[\text{MP-8}] - 1.6\,(\pm 2) \quad (10)$$

(iv) The efficiency of $ABTS^{+\bullet}$ formation decreased with increasing [H_2O_2] at constant [MP-8] (Figure 5).

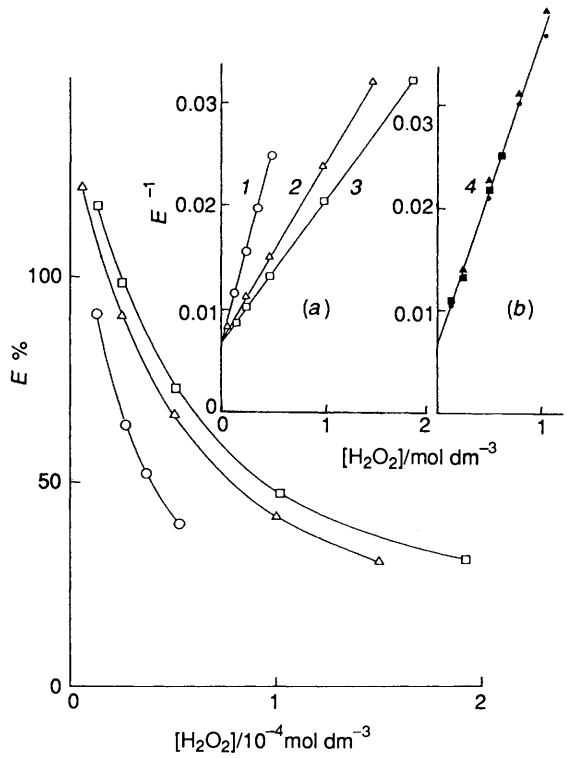

Figure 5. Plot of efficiency of [$ABTS^{+\bullet}$] formation *vs.* [H_2O_2] for three sets of data; [MP-8] 5 × 10^{-7} mol dm^{-3} in all cases: (□) [ABTS] 5 × 10^{-3} mol dm^{-3}; (△) [ABTS] 3 × 10^{-3} mol dm^{-3}; and (○) [ABTS] 0.5 × 10^{-3} mol dm^{-3}. Inset (*a*) to the Figure shows the accurately straight-line behaviour of plots of $1/E$ *vs.* [H_2O_2] for these [ABTS]; this allows evaluation of E_0—see the text. Inset (*b*) shows the invariance of both slope and intercept of $1/E$ *vs.* [H_2O_2] plots with [MP-8] data; [MP-8] 1.243 (▲); 2.485 (■); and 4.97 (●) × 10^{-7} mol dm^{-3}, respectively. The observed values for the slopes of lines 1–4 [insets (*a*) and (*b*)] are 368 (363); 154 (160); 114 (124); and 284 (270), respectively. Values in brackets are those calculated using E_0 143%, see the text.

(v) At constant [MP-8] the slope (sl) and intercept (k_0) of the straight-line variation of k_{obs} with [H_2O_2] varied with [ABTS] (Figure 6). The concentration dependence of sl and k_0 was accurately modelled by equations of the form (11) and (12).

$$\text{sl} = \frac{a[\text{MP-8}]}{b + [\text{ABTS}]} \quad (11)$$

$$k_0 = [\text{MP-8}]\left(k^* - \frac{c[\text{ABTS}]}{d + [\text{ABTS}]}\right) \quad (12)$$

Figure 7(*a*) and (*b*) demonstrates this dependence; in the first case, a, the straight-line nature of the plot of [MP-8]/Sl *vs.* [ABTS] demonstrates adherence to equation (11) with *a* 1.486 (±0.03) × 10^5 dm^3 mol^{-1} s^{-1}; *b* 2.82 (±0.07) × 10^{-4} mol dm^{-3}; while in the second, b, the solid line is the best-fit non-linear least-squares regression of equation (12) to the experimental k_0/[MP-8] data points shown. The derived parameter values for Figure 7(*b*) are k^* 4 778 (±81) dm^3 mol^{-1} s^{-1}; *c* 3 694 (±98) dm^3 mol^{-1} s^{-1}; *d* 1.081 (±0.08) 10^{-3} mol dm^{-3}.

(vi) The effect of bromide and formate ion on the kinetics of $ABTS^{+\bullet}$ formation was investigated to assess the effect of hydroxyl-radical scavengers on the reaction. The results, shown in the Table, indicate that Br^- has no significant effect on the efficiency of the reaction up to a concentration of 0.05 mol dm^{-1}; however, increasing the concentration of Br^- significantly increased k_{obs}.

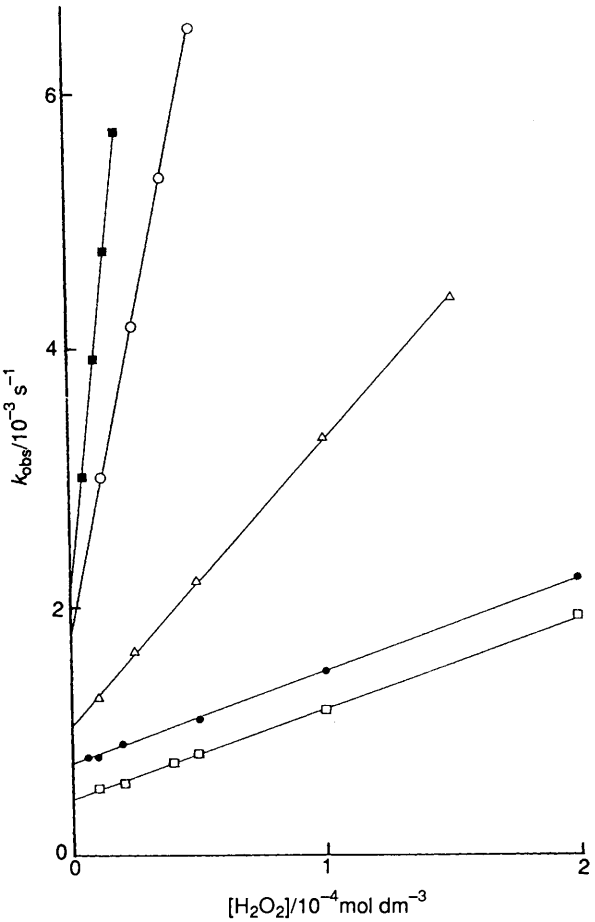

Figure 6. Plots of k_{obs} *vs.* $[H_2O_2]$ at several fixed concentrations of ABTS. [MP-8] 5×10^{-7} mol dm^{-3}; (●); (△); (○); and (■) were [ABTS] 1×10^{-2}; 3×10^{-3}; 5×10^{-4}; and 1.36×10^{-4} mol dm^{-3}, respectively; [MP-8] 2.5×10^{-7} mol dm^{-3}: (□) is [ABTS] 5×10^{-3} mol dm^{-3}.

Formate ion was observed to be without effect on either k_{obs} or efficiency at concentrations up to 0.10 mol dm^{-3}.

(vii) Spectrophotometric titration of MP-8 (1.1×10^{-6} mol dm^{-3}) with ABTS was carried out to investigate the possibility that ABTS may be a ligand of the haem peptide—this possibility was suggested by previous spectrophotometric evidence suggesting complex formation between ABTS and horseradish peroxidase.[6] The results shown in Figure 8 and inset suggest that a 1:1 complex between ABTS and MP-8 is indeed formed with a $K_d \sim 0.89 (\pm 0.05) \times 10^{-3}$ mol dm^{-3}.

Discussion

Preliminary studies of the use of ABTS as a chromophoric reducing substrate with which to monitor the MP-8-catalysed reduction of H_2O_2 indicated that rate constants obtained for this system, which were approximately constant (*i.e.* showed a variation of several tens of percent over a concentration range variation of several hundred percent or greater) may have been subject to subtle systematic non-random concentration variation. For this reason, particular care has been exercised to maximise the precision and reproducibility of the rate-constant data obtained spectrophotometrically, and we note that the precision of the rate-constant determination attained in this work (SD of the order of 1%) approaches that attained conductimetrically for the solvolysis of t-butyl chloride, at present the most precise solution kinetic data available.[22]

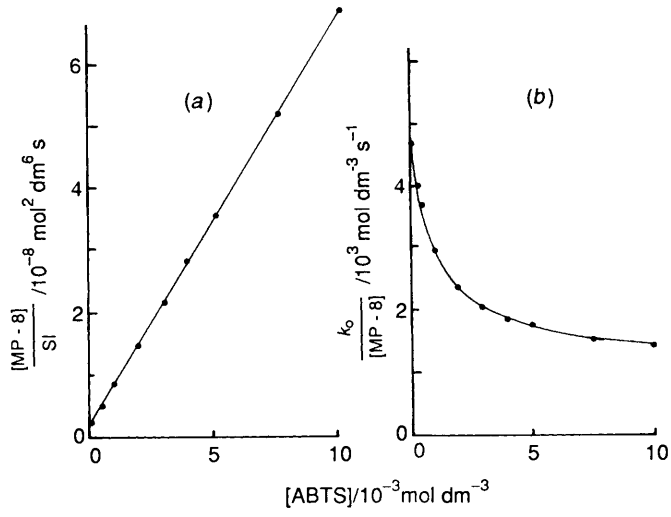

Figure 7. (*a*) Reciprocal plots of [MP-8]/Sl *vs.* [ABTS] to demonstrate the relationship (11) between the slope of the plots in Figure 6 and [ABTS] (*b*) Plot of k_0/[MP-8] *vs.* [ABTS], demonstrating the hyperbolic dependence on ABTS of the H_2O_2-independent component of k_{obs}. The solid line is that calculated using the least-squares parameter values given in the text for equation (12).

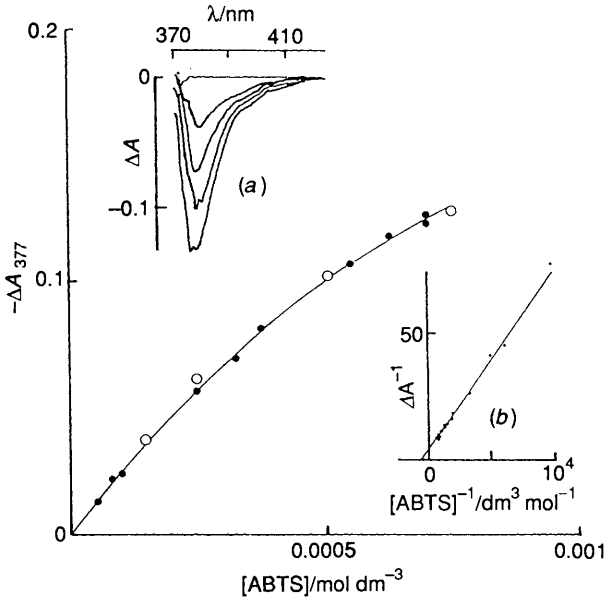

Figure 8. Spectrophotometric titration of MP-8 (1.1×10^{-6} mol dm^{-3} with ABTS at pH 7.00, *T* 25 (±1) °C. Inset (*a*) shows the difference spectrum observed with a ΔAbs decrease at 377 nm for the four data points shown as open circles, while the inset (*b*) demonstrates the hyperbolic nature of the $-\Delta A$ *vs.* [ABTS] curve. The solid line on the main Figure is that calculated assuming a 1:1 complex formation with K_d 0.89×10^{-3} mol dm^{-3}.

The first stage of the catalytic reaction between MP-8 and H_2O_2 (or HO_2^-)[14] must involve association between the two species to form the initial adduct $Fe^{3+}(H_2O_2/HO_2^-)$MP-8 (='A' in Schemes **a**–**c**). It is stressed that, in common with the work of other authors,[23] details of the complex structure, particularly with regard to electron distribution within the adduct, are deliberately unspecific.

The second catalytic step in the reaction is O–O bond cleavage, and, as noted by Bruice *et al.*,[8] this can proceed in two ways, either homolytically to give the hydroxyl radical (OH$^\bullet$)

and oxo-iron(IV)-porphyrin complex—an HRP compound II analogue, or heterolytically to give water plus an oxo-iron(IV)-porphyrin π cation radical species—an HRP compound I analogue. The products of either process would react with ABTS to give the $ABTS^{+\bullet}$ cation radical.

Two alternative minimum catalytic mechanisms can therefore be written—shown as Schemes **a** and **b**, respectively—to represent the two-equivalent reduction of H_2O_2 by ABTS in the presence of Fe^{3+}MP-8.

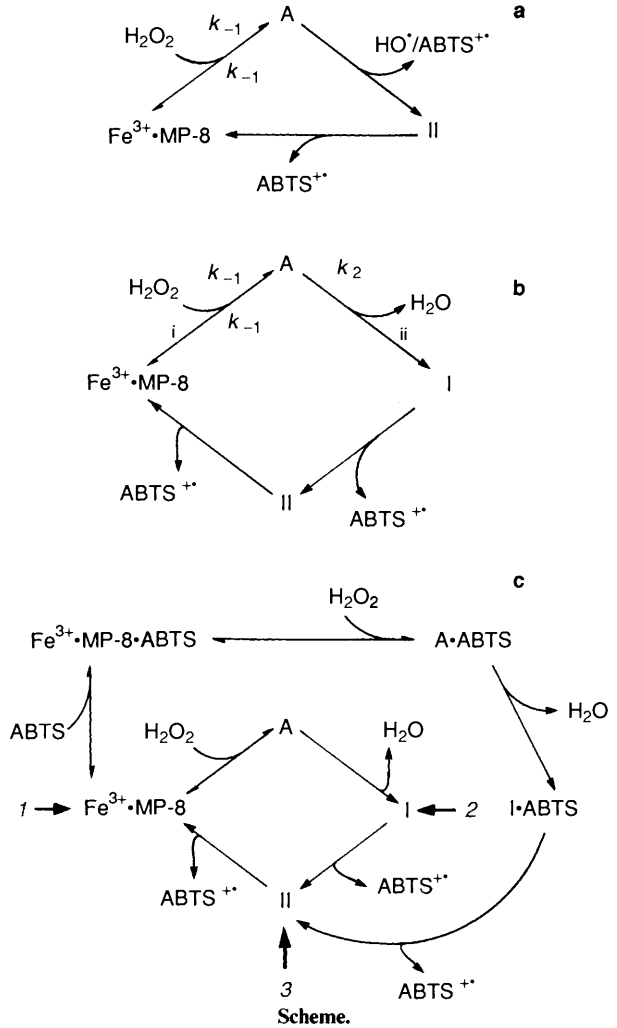

Scheme.

Obviously, a major discriminant between the two Schemes is the formation or absence of the hydroxyl radical during catalysis. Rush and Koppenol have utilised the yield of $ABTS^{+\bullet}$ in the presence or absence of bromide ion as a major criterion for determining OH• involvement in the catalytic reduction of H_2O_2 by iron nitrilotriacetate and ethylenediamine-*N*,*N*′-diacetate complexes.[21] In the presence of OH•, Br^- is quantitatively converted into the bromine radical $Br_2^{-\bullet}$ and, since OH• oxidises ABTS with an efficiency of 58% and $Br_2^{-\bullet}$ carries out the same reaction with an efficiency of ~90%,[24] an observed significant increase in $ABTS^{+\bullet}$ formation in the presence of Br^- argues in favour of Scheme **a**. Similarly the effect of formate—a powerful scavenger of hydroxyl radical—on the kinetics of $ABTS^{+\bullet}$ formation provides evidence for or against OH• formation during catalysis.[21]

The Table shows, in the case of Br^- addition, that the efficiency is unaffected at $[Br^-]$ up to 0.05 mol dm^{-3}, although a significant increase in k_{obs} occurs (Cl^- when used as a non-OH•-scavenging 'placebo' ion also causes a similar increase in k_{obs}, although only to the extent of *ca.* 50% that of Br^-); formate is without effect on either k_{obs} or the efficiency of $ABTS^{+\bullet}$ formation. These observations argue strongly against significant reduction of H_2O_2 *via* Scheme **a**, thus implying that the catalytic proceeds predominantly *via* route **b**.

The consistency of the observed kinetics of ABTS oxidation with Scheme **b** (subject to minor amendment) can now be demonstrated: the results of Figure 2(*a*) and (*b*) suggest the following rate law [equation (6′)]. Assuming that the reactions

$$d[ABTS^{+\bullet}]/dt = k[H_2O_2][MP\text{-}8] \qquad (6')$$

between ABTS and species I and II are very fast compared with steps (i) and (ii) (rate constants for the reaction of ABTS with a range of radical species are of the order of 10^9–10^{10} dm^3 mol^{-1} s^{-1})[24] a simple steady-state treatment of Scheme **b** under the assumption that $[H_2O_2] \gg [MP\text{-}8]$ shows the relevant rate law to be of the form (13) which, under the

$$(d[ABTS^{+\bullet}]/dt)_{t=0} = \frac{k_1k_2[MP\text{-}8][H_2O_2]}{[(k_{-1} + k_2) + k_1[H_2O_2]]} \qquad (13)$$

additional restriction $(k_{-1} + k_2) \gg k_1[H_2O_2]$—non-saturation of MP-8 by H_2O_2—reduces to the experimentally observed rate law.

In the system investigated here we have that $200 > [H_2O_2]/[MP\text{-}8] > 10$, and in all cases $ABTS^{+\bullet}$ formation was found to follow very precise pseudo-first-order kinetics over at least 90% reaction (see the Results section). A further requirement of non-saturation is that the experimentally observed first-order rate constant (k_{obs}) be:

(*a*) directly proportional to [MP-8], *i.e.* $k_{obs} = k[MP\text{-}8]$; and

(*b*) independent of $[H_2O_2]$;

in addition we have that:

(*c*) k_{obs} be independent of [ABTS]. This follows if the reaction of ABTS with I and II in Scheme **b** is very rapid compared with other reactions in the catalytic cycle.

The results shown in Figure 7(*a*) and (*b*) indicate that the pseudo-first-order rate constant for $ABTS^{+\bullet}$ formation is represented by the master equation (14) where *a*–*d* are given

$$k_{obs} = [MP\text{-}8]\left(k^* + \frac{a[H_2O_2]}{b + [ABTS]} - \frac{c[ABTS]}{d + [ABTS]}\right) \qquad (14)$$

as for equations (11) and (12). Use of these constants in equation (14) allowed calculation and comparison of the parameters expected for equations (7)–(10). Agreement is good; *e.g.* the calculated values for slope and intercept in equation (8) are 2.81×10^7 and 1 741 respectively.

From equation (14) at any constant $[H_2O_2]$ and [ABTS], requirement (*a*) above is satisfied up to [MP-8] 6×10^{-7} mol dm^{-3}, *i.e.* $k_{obs} = k[MP\text{-}8]$. Increasing deviation from strict proportionality above this concentration appears to be due to aggregation of MP-8 (monomer ~95% at 5×10^{-7} mol dm^{-3}; and ~85% at 1×10^{-6} mol dm^{-3}).[15] The limiting value of k_{obs} calculated at [ABTS] 5×10^{-3} mol dm^{-3} (1 741 dm^3 mol^{-1} s^{-1}) is in excellent agreement with the second-order rate constant calculated from the initial-rate studies at that concentration [Figure 2(*a*) and (*b*)], however, the experimentally observed dependence of k_{obs} on $[H_2O_2]$ and [ABTS] appears directly to contradict requirements (*b*) and (*c*) above. A degree of consistency can, however, be demonstrated by recognising that the structure of k_{obs} implies the existence of three independent parallel kinetic processes which can be considered separately.

First, we can dispense with the term independent of $[H_2O_2]$ and [ABTS], as that expected under non-saturation pseudo-first-order conditions for the catalytic cycle of Scheme **b**. The value of k^* (4 778 ± 87 dm^3 mol^{-1} s^{-1}) for this cycle compares

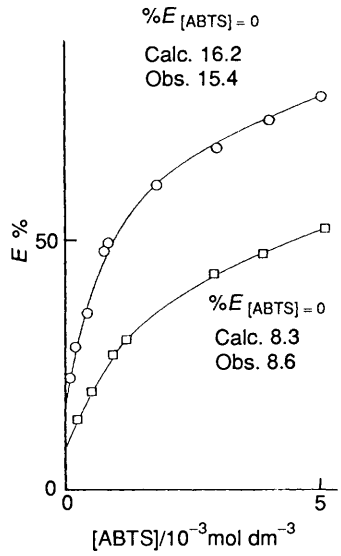

Figure 9. The effect of [ABTS] on E at [MP-8] 2.5×10^{-7} mol dm^{-3}; [H_2O_2] 1×10^{-4} mol dm^{-3} (□); and 4.66×10^{-5} mol dm^{-3} (○). The calculated values of $E_{[ABTS]=0}$ and those obtained by numerical extrapolation are indicated on the Figure.

well with the value of 5 290 (± 120) dm^3 mol^{-1} s^{-1}) obtained by Baldwin *et al.*[14] for the MP-8/H_2O_2 reaction at 25 °C, pH 7.0 ([PO_4^{3-}] 0.110) monitored using guaiacol as the reducing substrate.

The linear dependence of the second term of equation (14) on [H_2O_2] is consistent with direct degradative attack of H_2O_2 (or HO_2^-) on the catalytic centre of MP-8, namely the haem moiety. In support of this it is noted first, that oxidative degradation of iron-porphyrins by H_2O_2, in parallel with the catalytic reduction process, is well documented in the literature,[25] although the [H_2O_2] dependence found here indicates a direct degradative attack rather than an intra- or inter-molecular degradative process involving the active oxygen intermediates during the catalytic cycle.[26] Secondly, if catalytic and degradative pathways are operative then, at any particular constant [MP-8] and [ABTS], we deduce that the relative efficiency of the catalytic process is equal to the relative flux of H_2O_2 through the catalytic and degradative pathways respectively, *i.e.* equation (15) must hold, where E and k_{obs} are

$$E/E_0 = k_0/k_{obs} \qquad (15)$$

the efficiency and pseudo-first-order rate constants respectively at any given finite [H_2O_2], while E_0 and k_0 are the limiting efficiency and rate constant respectively at [H_2O_2] = 0. Equation (15) implies, since $k_{obs} = k_0 + k$[H_2O_2], that a plot of $1/E$ *vs.* [H_2O_2] be a straight line of intercept $1/E_0$ and slope k/E_0k_0; as shown in inset (*a*) to Figure 5 the above requirement holds accurately; a straight-line dependence of $1/E$ on [H_2O_2] was found in all cases studied and strongly supports the degradative hypothesis. Although the value of E_0 appeared to decrease slightly (to 131%) at the lowest [ABTS] studied it was found that the value was essentially invariant in the concentration range 2.5×10^{-4} mol dm^{-3} < [ABTS] < 1.0×10^{-2} with a mean value of 143 (± 2%). Further consequences of equation (15) are that E should be independent of [MP-8], and secondly that, as [ABTS] ⟶ 0, E should approach the limiting value E_0 (4 478/{4 778 + (1.486×10^5 [H_2O_2]/2.82×10^{-4}}). As shown in the inset (*b*) to Figure 5 both E_0 and k/k_0 (and thus E) are, as predicted, independent of [MP-8] in the range 1–5 $\times 10^{-7}$ mol dm^{-3}. Furthermore, numerical extrapolation of E to [ABTS] = 0 at two [H_2O_2] values (1 and 0.466×10^{-4} mol dm^{-3}) gave good agreement between $E_{calc}^{[ABTS]=0}$ and observed (Figure 9), as predicted above.

The inverse dependence on [ABTS] of the H_2O_2-dependent component is consistent with ABTS inhibition of H_2O_2-mediated degradation. A similar situation is found in the case of competitive inhibition in steady-state enzyme kinetics[27] where an equilibrium exists between enzyme and inhibitor (I) resulting in formation of a non-catalytically competent complex. Under conditions of non-saturation of enzyme by substrate, perturbation of the kinetics by a factor K_i (K_i + [I])$^{-1}$ (where K_i is the enzyme inhibitor dissociation complex) occurs. This suggests that ABTS forms a complex with MP-8 which cannot be degradatively attacked by H_2O_2. If the proposed MP-8·ABTS complex, which is suggested by the form of the H_2O_2-dependent term, possesses a significant catalytic activity—characterised by rate constant k', where k' is lower than the catalytic rate constant of free MP-8 (4 778 dm^3 mol^{-1} s^{-1}), then effectively two catalytic cycles will operate in parallel. As [ABTS] ⟶ 0 and in the limit [H_2O_2] = 0, k_{obs}/[MP-8] will approach k^*; alternatively, as [ABTS] ⟶ ∞, k_{obs} will approach the lower limiting value k'. Furthermore, the approach to this lower value would be expected (subject to the usual concentration and rate requirements) to follow an inverse (in the sense of decreasing) saturation rate law, *i.e.* at any particular [ABTS] the value of k_{obs} would be less than k^* by a factor c[ABTS]/(d + [ABTS]), where c is the difference between k^* and k', and d is the dissociation constant of the MP-8·ABTS complex. As can be seen from equation (14) this is precisely the situation which exists, the value of d (1.081×10^{-3} mol dm^{-3}) found experimentally being in good agreement with the value of K_d (0.89×10^{-3} mol dm^{-3}) obtained by non-kinetic means, *i.e.* spectrophotometric titration (Figure 8). The value of k'—the limiting rate constant for catalysis *via* the MP-8·ABTS pathway—obtained here is 1 084 dm^3 mol^{-1} s^{-1} and is almost identical with the second-order rate constant for ABTS oxidation (~1 000 dm^3 mol^{-1} s^{-1}) interpolated at pH 7 from the data (Figure 1) of Bruice *et al.*,[8] on the non-buffer-catalysed reduction of H_2O_2 by a monomeric iron-porphyrin in aqueous solution.

In conclusion it has been demonstrated by precise kinetic studies that the MP-8-catalysed reduction of H_2O_2 by ABTS is complex. Consistency of the kinetics with two parallel catalytic cycles (involving free MP-8 and an MP-8·ABTS complex, respectively) has been demonstrated, the MP-8-catalysed cycle being susceptible to oxidative degradative attack by H_2O_2, while the MP-8·ABTS cycle is not. These conclusions are summarised by the composite catalytic cycle shown in Scheme **c** where the possible points of degradative attack for H_2O_2 during the MP-8 catalytic cycle are shown by arrows 1–3.

Assuming the correctness of the parallel MP-8 and MP-8·ABTS complex pathway hypothesis we can immediately rule out H_2O_2 attack at point *3*, *i.e.* on the compound II analogue, since it is common to both cycles. This leaves either attack of H_2O_2 on the compound I analogue (point *2*) or directly on MP-8 (point *1*); however, only attack at point *2* would lead to a product term [MP-8][H_2O_2] in the expression for k_{obs}, given non-saturation of the haem by H_2O_2 and the very rapid reaction of ABTS with I and II. This is in agreement with recent studies by Bretcher and Jones[28] who implicated nucleophilic attack by water at the porphyrin *meso* position of the compound I analogue in oxidative catalyst destruction during reaction of coprohaem with peroxy acids.

References

1 D. Portsmouth and E. A. Beal, *Eur. J. Biochem.*, 1971, **19**, 479.
2 S. B. Brown, P. Jones, and A. Suggett, *Trans. Faraday Soc.*, 1968, **64**, 721.

3 S. B. Brown and H. Hatzikonstantinou, *Biochim. Biophys. Acta*, 1979, **585**, 143.
4 T. G. Traylor, W. A. Lee, and D. V. Stynes, *J. Am. Chem. Soc.*, 1984, **106**, 755.
5 T. G. Traylor, W. A. Lee, and D. V. Stynes, *Tetrahedron*, 1984, **40**, 553.
6 R. E. Childs and W. G. Bardsley, *Biochem. J.*, 1975, **145**, 93.
7 M. F. Zipplies, W. A. Lee, and T. C. Bruice, *J. Am. Chem. Soc.*, 1986, **108**, 4433.
8 T. C. Bruice, M. F. Zipplies, and W. A. Lee, *Proc. Natl. Acad. Sci. USA*, 1986, **83**, 4646.
9 A. Ehrenberg and H. Theorell, *Acta Chem. Scand.*, 1955, **9**, 1193.
10 Y. Baba, H. Mizushima, and H. Watanabe, *Chem. Pharm. Bull.*, 1969, **17**, 82.
11 H. Plattner, E. Wachter, and P. Gröbner, *Histochemistry*, 1977, **53**, 223.
12 N. Ghinea and N. Simoneson, *J. Cell. Biol.*, 1985, **100**, 606.
13 H. M. Marques, Ph.D. Thesis, University of the Witwatersrand, Johannesburg, South Africa, 1986.
14 D. A. Baldwin, H. M. Marques, and J. M. Pratt, *J. Inorg. Biochem.*, 1987, **30**, 203.
15 J. Aron, D. A. Baldwin, H. M. Marques, J. M. Pratt, and P. A. Adams, *J. Inorg. Biochem.*, 1986, **27**, 227.
16 D. A. Baldwin, H. M. Marques, and J. M. Pratt, *J. Inorg. Biochem.*, 1986, **27**, 245.
17 P. A. Adams and R. D. Goold, *J. Chem. Soc., Chem. Commun.*, 1990, 97.
18 D. P. Nelson and L. A. Kiesow, *Anal. Biochem.*, 1972, **39**, 474.
19 P. A. Adams, M. P. Byfield, R. D. Goold, and A. E. Thumser, *J. Inorg. Biochem.*, 1989, **37**, 55.
20 P. A. Adams, C. Adams, and D. A. Baldwin, *J. Inorg. Biochem.*, 1986, **28**, 441.
21 J. D. Rush and W. H. Koppenol, *J. Am. Chem. Soc.*, 1988, **110**, 4957.
22 M. J. Blandamer and J. W. M. Scott, *J. Phys. Chem.*, 1988, **92**, 6266.
23 H. K. Baek and H. E. Van Wart, *Biochemistry*, 1989, **28**, 5714.
24 B. S. Wolfendon and R. L. Willson, *J. Chem. Soc., Perkin Trans. 2*, 1982, 805.
25 P. Jones, K. Prudhoe, and T. Robson, *Biochem. J.*, 1973, **135**, 361.
26 S. B. Brown, *Biochem. J.*, 1976, **159**, 23.
27 I. H. Segal, 'Enzyme Kinetics,' Wiley, New York/Chichester/Brisbane/Toronto, 1975.
28 K. R. Bretscher and P. Jones, *J. Chem. Soc., Dalton Trans.*, 1988, 2273.

Paper 9/05164C
Received 6th *December* 1989
Accepted 22nd *March* 1990